Journal of Thermal Analysis and Calorimetry, Vol. 87 (2007) 3, 725–730

$BaTi_{1-x}Zr_xO_3$ NANOPOWDERS PREPARED BY THE MODIFIED PECHINI METHOD

*M. I. B. Bernardi**, *E. Antonelli, A. B. Lourenço, C. A. C. Feitosa, L. J. Q. Maia and A. C. Hernandes*

Grupo Crescimento de Cristais e Materiais Cerâmicos, Instituto de Física de São Carlos, Universidade de São Paulo
Cx. P.: 369 CEP 13560 970, São Carlos, SP, Brazil

The results reported here based on a study of $BaTi_{1-x}Zr_xO_3$ (x=0, 0.2 and 1) nanometric powders prepared by the modified Pechini method. The powder samples annealed from 600 to 1000°C/2 h were characterized by thermogravimetric analysis (TG), differential scanning calorimetry (DSC), X-ray diffraction (XRD) and scanning electron microscopy (SEM) techniques. The decomposition reactions of resins were studied using thermal analysis measurements. The barium titanate zirconate system presented just one orthorhombic phase. Furthermore, this study produced $BaTiO_3$ powders with a tetragonal structure using shorter heat treatments and less expensive precursor materials than those required by the traditional methods.

Keywords: *$BaTi_{1-x}Zr_xO_3$, nano-powder, Pechini method*

Introduction

Solid solutions based on barium titanate ($BaTiO_3$) offer a large range of possible property modification. Recently, $Ba(Zr_xTi_{1-x})O_3$ (BTZ) system has been established as one of the most important compositions for dielectrics in multilayer capacitors [1]. At a Zr content less than 10 at%, BZT ceramics show a normal ferroelectric behavior and dielectric anomalies corresponding from cubic to tetragonal (Tc), tetragonal to orthorhombic (T2) and orthorhombic to rhombohedral (T3) phases transitions, have been unequivocally identified. At around 27 at%, Zr-doping BZT ceramics exhibit typical diffuse paraelectric to ferroelectric phase transition behavior, whereas Zr-richer compositions display typical relaxor-like behavior in which Tc shifts to higher temperatures with increased frequencies [1–3].

The grain size influence on the electrical performance has been extensively studied [4–6] and there is consensus that the dielectric constant optimal value occurs for fine-grained and dense material. Therefore, microstructure controlling is the key to the enhancing electrical performance of ceramics, and can only be done by using a non-conventional preparation method.

Obtainment of $BaTiO_3$ nanometric particles has been widely studied by several chemical methods, such as thermal decomposition of coprecipitated barium titanate oxalate [7], sol–gel [8–10], hydrothermal [11, 12] and polymeric precursors based on the Pechini-type process [13–19]. However, a few works have been focused in the synthesis of the BTZ powders through chemical methods [2, 20].

BTZ is conventionally produced by solid-state reactions between $BaCO_3$, TiO_2 and ZrO_2 at high temperatures (>1200°C) [21]. Nevertheless, the conventional method is not suitable due to problems involving interparticle sintering and contamination during the calcination and milling steps required [22]. Larger control of the stoichiometry, lower synthesis temperatures, and the easy introduction of dopants has rendered the polymeric precursor process to be more advantageous than the mixed-metal oxides synthesis method.

Based on these trends, the purpose of this work was the application of the thermal analysis techniques as basic tools for the identification of thermal events during the calcination. Thus, making possible the BTZ nanometric powders preparation at low temperatures using an unaggressive and inexpensive chemical method. We have also employed XRD and SEM to determine the crystalline phases and microstructure of the powders, respectively.

Experimental

Flowchart in Fig. 1 illustrates the procedure employed in the preparation of $BaTi_{1-x}Zr_xO_3$ (x=0, 0.2, 0.8 and 1) powders, while Table 1 lists the origin and purity of the precursor materials. The synthesis was carried out by the polymeric precursor method using an aqueous metals citrate solution prepared from $Zr(OC_3H_7)_4$ and $Ti(OC_3H_7)_4$ and citric acid with a cit-

* Author for correspondence: m.basso@if.sc.usp.br

1388–6150/$20.00

Akadémiai Kiadó, Budapest, Hungary
Springer, Dordrecht, The Netherlands

Table 1 Materials used in the synthesis of $BaTi_{1-x}Zr_xO_3$

Reagent	Chemical formula	Source	Purity/%
Zirconium isopropoxide	$Zr(OC_3H_7)_4$	Alfa Aesar	97
Titanium isopropoxide	$Ti(OC_3H_7)_4$	Alfa Aesar	97
Citric acid monohydrate	$C_6H_8O_7 \cdot H_2O$	Synth.	99
Ethylene glycol	$C_2H_6O_2$	Mallinckrott	99.9
Barium acetate	$(CH_3COO)_2Ba$	Baker Analyzed	99

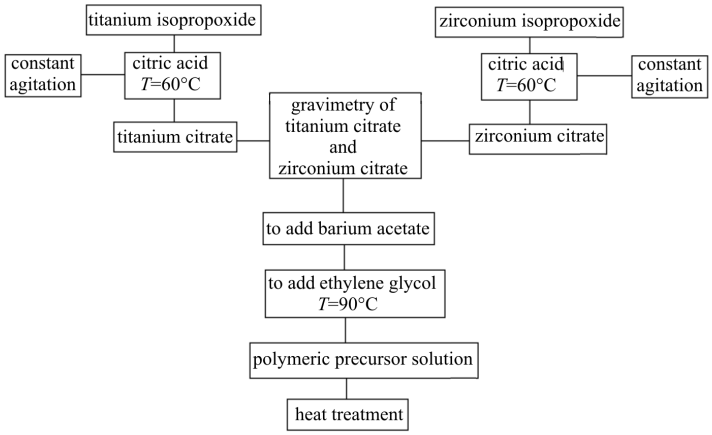

Fig. 1 Flowchart of the preparation of $BaTi_{1-x}Zr_xO_3$ nanometric powder using the polymeric precursor method

ric acid (CA)/metal (ME) ratio of 3.5:1 (in mol). Barium acetate precursor was added slowly. Ethylene glycol (EG) was added to the citrate solution at a mass ratio of 40:60 in relation to the citric acid to promote polymerization reactions. The pH was adjusted to 3–4 with ethylenediamine, depending on the composition. Finally, the complete dissolution of the salts resulted in a stable clear solution (resin) for four years.

Thermal analyses were made based on thermogravimetry (TG) and differential scanning calorimetry (DSC) techniques, (Netzsch STA 409C), under synthetic air (O_2/N_2=1/4) at a flow rate of 80 mL min^{-1} and a heating rate of 10°C min^{-1}. Al_2O_3 was used as reference material and for sample holders. No previous treatment was performed in the polymeric resin before the thermal analysis measurements.

The crystalline phase measurements were based on X-ray diffraction (XRD) patterns obtained at room temperature, using a Rigaku Geigerflex diffractometer with CuK_α radiation (λ=1.5406 Å, a scan rate of 2° min^{-1} and 2θ=20 to 60°).

The powder morphology was examined by scanning electron microscopy (SEM) (Zeiss DSM 960 model, Germany).

Results and discussion

The thermal decomposition events occurring on BZT resins were a multistage complex process involving at least five mechanisms. Figures 2a–c illustrate the curves obtained from the resins with different compositions performed using TG and DSC techniques. DTG curves are presented in Fig. 2 while Table 2 lists the mass losses in various temperature ranges. Two endothermic reactions occurred in the temperature ranging from 25 to 200°C due to resin dehydration at 100°C from absorbed water, and at 170°C from structural water, leading a loss mass around 18–31%. Between 200–400°C the sample undergoes successive exothermal reactions, with loss mass varying from 27 to 61%, indicating the process of pyrolysis. Two exothermic overlapped reactions were observed in the 400–550°C temperature range, which was a result of the material oxidation and which led to a mass loss ranging from 15 to 20%. The decomposition of residual CO_2 and formation of the crystalline phase occurred between 550 and 700°C with a mass loss around 1–4%.

Only the $BaTiO_3$ sample exhibited a mass loss from 6 to 7% above 700°C, with an exothermic reaction with a peak maximum at 773°C. This peak in the $BaTiO_3$ composition was caused by both a cubic to tetragonal phase transition and the mass loss. This mass loss was related to the elimination of residual carbon in the sample. The other compositions showed no reaction or mass loss above 600°C. We believed that this fact was induced due to the Zr presence in polymeric chair and the ethylenediamine used for pH control.

Therefore, we have performed the heat treatment in two stages: initial heating at 300°C for 5 h at a heat-

Table 2 Thermal analysis data of resins

Composition	Dehydration/%	Oxidation decomposition/%		Decomposition of residueal CO_2/phase formation/%	
	25–200°C	200–400°C	400–550°C	550–700°C	700–1000°C
$BaTiO_3$	27	27	20	1	7
$BaTi_{0.8}Zr_{0.2}O_3$	31	34	19	4	0
$BaZrO_3$	18	61	16	1	0

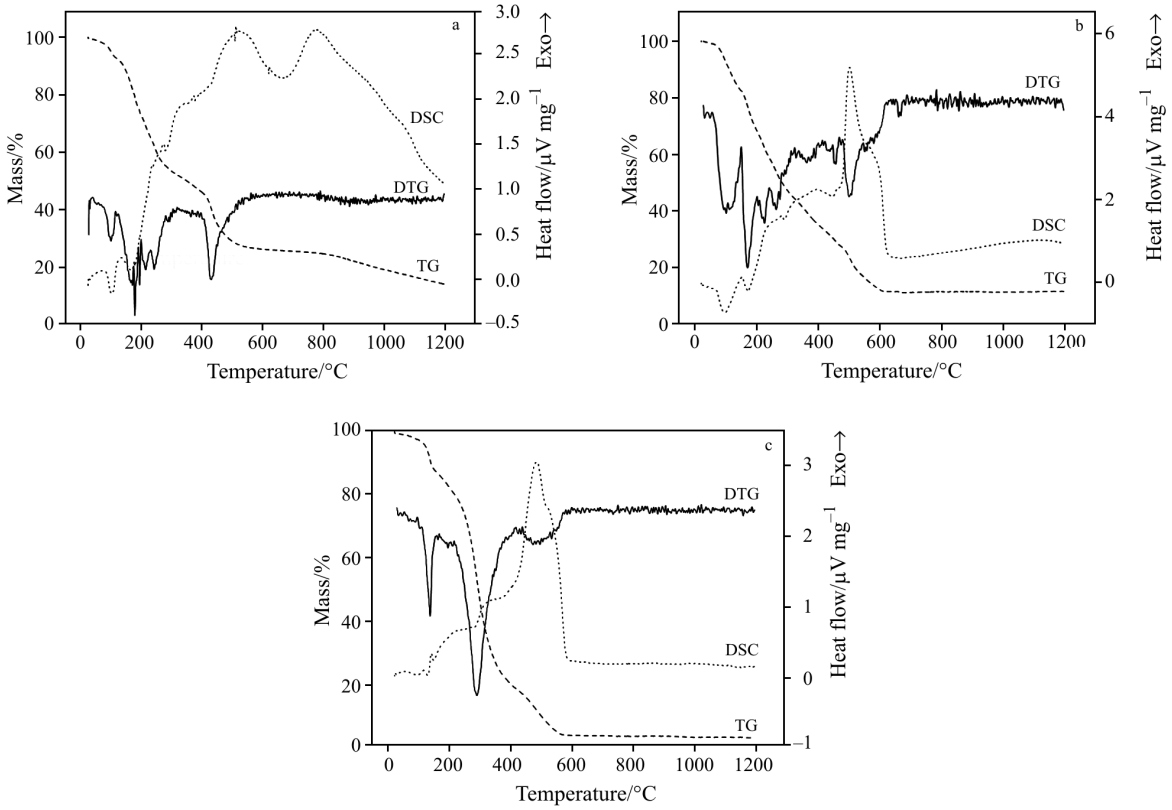

Fig. 2 Simultaneous DSC/TG-DTG curves of the resin obtained by the Pechini method: a – $BaTiO_3$, b – $BaTi_{0.8}Zr_{0.2}O_3$ and c – $BaZrO_3$ systems

ing rate of 10°C min^{-1} for pyrolysis of organic materials, followed by powder pulverization using an agate mortar and sieving through a 100 mesh sieve. The second stage consisted of heat treatments ranging from 600 to 1000°C for 2 h, using a 10°C min^{-1} heating rate, followed by their XRD measurements.

Figures 3a–c show the diffraction patterns of the powder systems studied in a temperature ranging from 600 to 1000°C. The $BaTiO_3$ system presents a cubic phase at 800°C. A transition from cubic to tetragonal phase occurred between 800 and 900°C, with complete conversion of the powders to the tetragonal phase occurring at 900°C/2 h. The $BaTiO_3$ remained tetragonal up to 1000°C and stabilized at room temperature, corroborating with DSC results. This tetragonal phase displayed ferroelectric properties as described by Arima *et al*. [23], who obtained the same phase at 900°C/8 h using the polymerized complex method based on the Pechini-type reaction route.

We believe that the difference in time at the temperature of 900°C between our results and that of Arima *et al*. [23] is attributed to the molar ratio used between of citric acid, metal and ethylene glycol. In this work, we have used the molar ratio of CA:EG:ME=3.5:0.7:1, while Arima *et al*. [23] have used CA:EG:ME=5:20:1. Then, we used a smaller content of citric acid and ethylene glycol. Therefore, our resin possesses a smaller organic material quantity to eliminate during the pyrolysis, leading at lower calcination temperature and phase formation. Probably, our ratio promotes a chemical structure in which the metals are more closed and better arranged. Mohallem [24] has obtained a tetragonal phase at 900°C/2 h using the sol–gel method, while Rayendran *et al*. [25] pro-

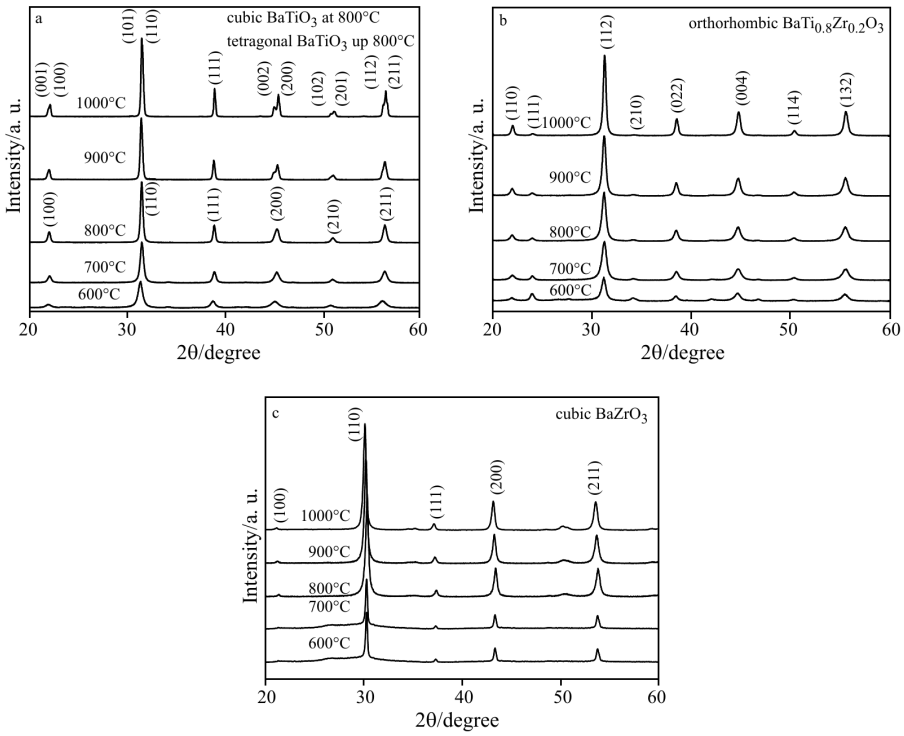

Fig. 3 XRD pattern of the powder heat treated between 600 to 1000°C for 2 h: a – $BaTiO_3$, b – $BaTi_{0.8}Zr_{0.2}O_3$ and c – $BaZrO_3$ systems

duced the same phase at 1050°C/24 h using the oxide mixture method. As it can be seen, in this study we have produced $BaTiO_3$ powders with a tetragonal structure using shorter heat treatments and less expensive precursor materials than those required by the traditional methods. Due to this phase transition, a reduction in the material crystallinity was observed at 900°C (Fig. 4) resulting from the system transformation cubic to tetragonal phase, with a higher relative crystallinity at 1000°C. The barium titanate zirconate systems in the various stoichiometries presented just one orthorhombic phase, which was generated, according to the crystallographic card (code 88537-ICSD collection) [26, 27], from the $BaTi_{1-x}Zr_xO_3$ (x=0.2) system.

A significant fact revealed by these XRD patterns is that the diffraction peaks shifted to lower angles as the Zr content increased. This shift is illustrated in Fig. 5, which showed the (110) diffraction peak of $BaTiO_3$/$BaZrO_3$ and the (112) diffraction peak of $BaTi_{0.8}Zr_{0.2}O_3$ powders. This peak shifting indicates an increase in the lattice parameter, which was expected since the ionic radius of Zr^{4+} (0.86 Å) is larger than Ti^{4+} (0.745 Å), in agreement with Dixit *et al*. [5], who prepared the Zr-doped $BaTiO_3$ thin films by the sol–gel technique.

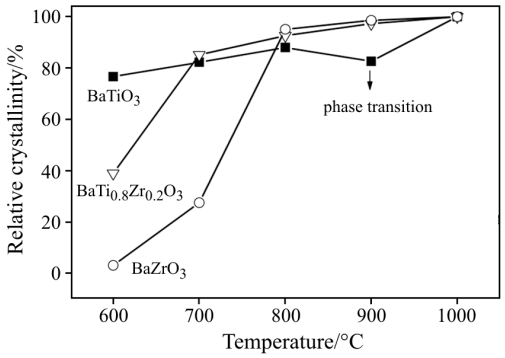

Fig. 4 Relative crystallinity of $BaTi_xZr_{1-x}O_3$ powders as a function of the heat treatment

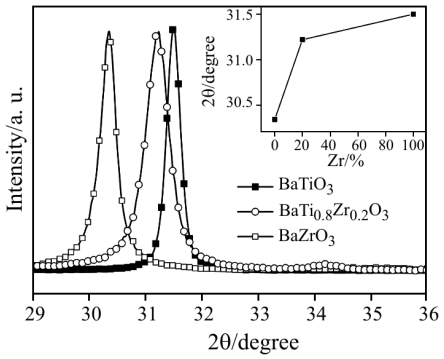

Fig. 5 Shift of the (112) and (110) diffraction peaks of $BaTi_xZr_{1-x}O_3$ powders with increasing Zr content

Figure 6 shows the crystallite and the particle sizes of the calcined powders at 800°C/2 h as a function of the Zr content. The crystallite sizes were evaluated through the Scherrer equation [26], and the average particle sizes were determined from the FE-SEM images (see insert in Fig. 6). It is known that powders with nanometric grains are thermodynamically unstable due to the large surface area. That means that the small dimension grains have a high surface energy leading to the powder agglomerate. This behavior can be visualized in our SEM micrographs. The average particle size of these powders is about 150 nm and exhibits homogeneous distribution of the size and shape. Both crystallite and particle size present similar behavior. The Zr content did not cause the grain size variation in the powders. This behavior is also observed in the crystallite size which presents about a 30 nm size.

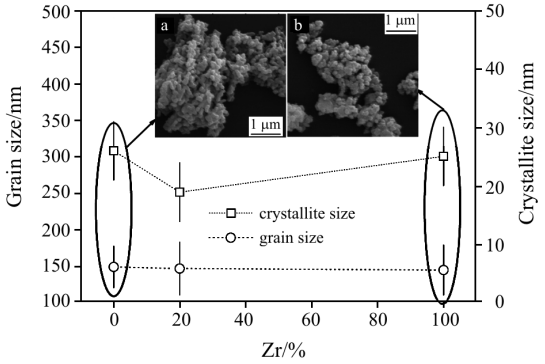

Fig. 6 Crystallite and particle size dependence with the Zr value for the samples calcined at 800°C/2 h. The insert in Fig. 6 presents SEM micrograph of the powder: a – $BaTiO_3$ and b – $BaZrO_3$ systems

Our results indicate that under specific compositions by the method studied here, it is possible to establish the orthorhombic phase for BTZ compositions. Here only XRD results are presented on $BaTi_{0.8}Zr_{0.2}O_3$. However, the $BaTi_{0.2}Zr_{0.8}O_3$ composition shows also the orthorhombic structure for heat treatments ranging from 600 to 1000°C (results not presented in this work). Then, in these cases the BTZ ferroelectric ceramic can display typical relaxor-like behavior.

Conclusions

Thermal analysis was indispensable to determine the thermal events, decomposition, phase formation and structural transformation. $BaTi_{1-x}Zr_xO_3$ ceramic powders were prepared with x=0, 0.2 and 1 compositions using the polymeric precursor method, where homogeneous, highly pure powders were obtained. These powders were heat-treated at relatively low temperatures, and shorter calcination times were applied compared to other authors. The tetragonal phase of the $BaTiO_3$ system, which displayed highly interesting ferroelectric properties for electronic applications, was obtained at 900 and at 1000°C/2 h. The composition containing Ti and Zr presented an orthorhombic structure in every studied temperature range. This structure was obtained at temperatures as low as 600°C. The replacement of Ti by Zr did not cause grain size variation.

Acknowledgements

The authors gratefully acknowledge the financial support of the Brazilian research funding institution FAPESP, and their indebtedness to Dr. Antonio Carlos Doriguetto for his stimulating discussions on the crystallographic results.

References

1 J. Bera and S. K. Rout, Mater. Lett., 59 (2005) 135.
2 X. G. Tang, J. Wang, X. X. Wang and H. L. W. Chan, Solid State Commun., 131 (2004) 163.
3 P. S. Dobal, A. Dixit and R. S. Katiyar, J. Appl. Phys., 89 (2001) 8085.
4 G. Arlt, D. Hennings and D. With, J. Appl. Phys., 58 (1985) 1619.
5 A. Dixit, S. B. Majumder, A. Savvinov, R. S. Katijar, R. Guo and A. S. Bhalla, Mater. Lett., 56 (2002) 933.
6 S. Aoyagi, Y. Kuroiwa, A. Sawada, H. Kawaji and T. Atake, J. Therm. Anal. Cal., 81 (2005) 627.
7 M. Stockenhuber, H. Mayer and J. Alercher, J. Am. Ceram. Soc., 76 (1993) 1185.
8 M. N. Frey and D. A. Payne, Chem. Mater., 7 (1995) 123.
9 G. Pfaff, J. Mater. Sci., 2 (1992) 591.
10 H. B. Sharma, R. P. Tandon, A. Mansingh and R. Rup, J. Mater. Sci. Lett., 12 (1993) 1795.
11 L. Zhao, A. T. Chien, F. F. Lange and J. S. Speck, J. Mater. Res., 11 (1996) 1325.
12 Y. S. Her and E. Matijevic, J. Mater. Res., 10 (1995) 3106.
13 V. Vinothini, P. Singh and M. Balasubramanian, Ceram. Int., 32 (2006) 99.
14 S. Kumar, G. L. Messing and W. B. White, J. Am. Ceram. Soc., 76 (1993) 617.
15 D. Hennings and W. Mayr, J. Solid State Chem., 26 (1978) 329.
16 M. P. Pechini, Method of preparing lead and alkaline earth titanates and niobates coating method using the same to form a capacitor, US PAT., 3.330.697, 1967.
17 E. Antonelli, R. S. Silva and A. C. Hernandes, Ferroelectrics, (2006), accepted.
18 E. Antonelli, M. I. B. Bernardi and A. C. Hernandes, Cerâmica, 51 (2005) 430.
19 M. A. F. Souza, A. G. Souza, R. A. Candeia, D. M. A. Melo, L. E. B. Soledade, M. R. C. Santos, I. M. G. Santos, S. J. G. Lima and E. Longo, J. Therm. Anal. Cal., 79 (2005) 411.

20 M. Veith, S. Mathur, N. Lecerf, V. Huch, T. Decker, H. P. Beck, W. Eiser and R. Haberkorn, J. Sol-Gel Sci. Technol., 15 (2000) 145.
21 J. Bera and S. K. Rout, Mater. Lett., 59 (2005) 135.
22 J. Moon, E. Suvaci, T. Li, S. A. Costantino and J. H. Adair, J. Eur. Ceram. Soc., 22 (2002) 809.
23 M. Arima, M. Kakihana, Y. Nakamura, M. Yashima and M. Yoshimura, J. Am. Ceram. Soc., 79 (1996) 2847.
24 N. D. S. Mohallem, 'Preparação de pós e filmes finos de $BaTiO_3$ pelo método sol-gel', Ph.D. Thesis, Universidade de São Paulo, São Carlos, Brazil 1990.
25 M. Rajendran and M. S. Rao, J. Solid State Chem., 113 (1994) 239.
26 J. Joseph, T. M. Vimala, J. Raju and V. R. K. Murthy, J. Phys. D: Appl. Phys., 32 (1999) 1049.
27 H. P. Klug and L. E. Alexander, 'X-ray Diffraction Procedures: for Polycrystalline and Amorphous Materials', John Wiley & Sons, USA 1954, p. 410.

DOI: 10.1007/s10973-006-7767-z